Adv. Studies Theor. Phys., Vol. 3, 2009, no. 9, 333 - 352

Effect of the Moving Force on the Radiated Sound from Rectangular Plates with Elastic Support

Yufeng Qiao* and Qibai Huang

School of Mechanical of Science & Engineering
Huazhong University of Science & Technology
Wuhan 430074, China
*Corresponding Author. Tel: +86-27-8755-7664
E-mail Address: yufengqiao@gmail.com

Abstract

The effect of the moving force on the radiated sound from the rectangular plates with elastic support is revealed in this paper. An analytical method in conjugation with numerical method is also developed to calculate the sound radiated from the plates. According to this method, the radiated sound is calculated for rectangular plate with different elastic support boundary conditions. By comparing these calculation results, the effect of the elastic support on the radiated sound is also studied. Moreover, the effect of the plate mode density is included in the research results.

Keywords: Radiated Sound, Rectangular Plates, Elastic Support, Moving Force

1. Introduction

Rectangular and rectangular-like plates with elastic-support are frequently encountered in mechanical product design. They often play the role of the main noise source of the product. Thus, control of the radiated noise from the plates becomes an important issue. Moving force is an ordinary form of force conditions in design. Therefore, it is necessary to obtain the effect of the moving force on the radiated sound from the rectangular plate with elastic support.

Since no analytical method exists to solve the forced response of the rectangular plate with elastic support, we have to adopt approximate solutions in conjunction with numerical methods. Different techniques have been developed to solve the problem in the past. These techniques include the spline technique [1], Galerkin's method [2], the finite strip method [3], the Ritz method [4] and the Rayleigh-Ritz method [5]. In fact, the force applied on the plate maybe a moving force. Therefore, it is also worth value to study the effect of the moving force on the radiated sound. Gbadeyan and Oni [6] studied the dynamic response of the rectangular plate excited by moving force. Takabatake [7] presented a simplified analytical method for the rectangular plate subjected to moving force to examine the effect of the additional mass due to moving force.

The purpose of this paper is to investigate the effect of the moving force on the radiated sound from the rectangular plate with elastic support. By comparing the boundary condition applied at different sides of the plates, the effect of the moving force and the elastic boundary on the radiated sound from the plate is studied.

2. Sound Radiation Governing Equations

Consider an elastically supported rectangular plate, which is shown in Fig.1, excited by a point force. The governing equation for the transverse displacement $w(x,y,t)$ is given by [8, 9]

$$D\nabla^4 w(x,y,t) + c_d \frac{\partial w(x,y,t)}{\partial t} + \rho h \frac{\partial^2 w(x,y,t)}{\partial t^2} = f(t). \quad (1)$$

Here D is the flexural rigidity defined by $D = Eh^3/12(1-\mu^2)$, E is the Young's modulus, h is the plate thickness, μ is the Poisson's ratio, c_d is the damping coefficient of the rectangular plate, $f(t)$ is the force applied on the plate, t is time, ρ is the mass density, $\nabla^4 = \nabla^2\nabla^2 = \frac{\partial^4}{\partial x^4} + 2\frac{\partial^4}{\partial x^2 \partial y^2} + \frac{\partial^4}{\partial y^4}$ and ∇^2 is the Laplace operator.

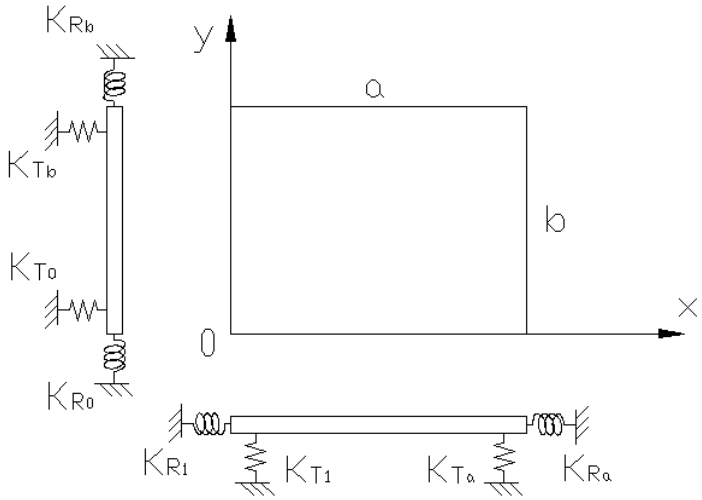

Figure.1 Rectangular plate with elastic support and coordinate system

For a harmonic excitation of circular frequency ω, we set

$$w(x,y,t) = W(x,y)e^{j\omega t}, \quad (2)$$

$$F(t) = Fe^{j\omega t}. \quad (3)$$

$W(x,y)$ can be written as the superposition of adequate shape functions

$$W(x,y) = \sum_{m=1}^{\infty}\sum_{n=1}^{\infty} W_{mn}\Phi_{mn}(x,y), \quad (4)$$

where $\Phi_{mn}(x,y)$ is the modal shape functions, W_{mn} is the displacement coefficient.

Consider a harmonic point force $f_m(t)$ that moves on the plate at speed of v_x and v_y, respectively, as shown in Fig.2. The moving force $f_m(t)$ can be expressed as

$$f_m(t) = F(t)\delta(x - x_0 - v_x t)\delta(y - y_0 - v_y t), \tag{5}$$

where $F(t)$ is the magnitude of the moving force, $\delta(x)$ and $\delta(y)$ are the Dirac Delta functions, (x_0, y_0) is the initial location that the moving force applies on the plate surface.

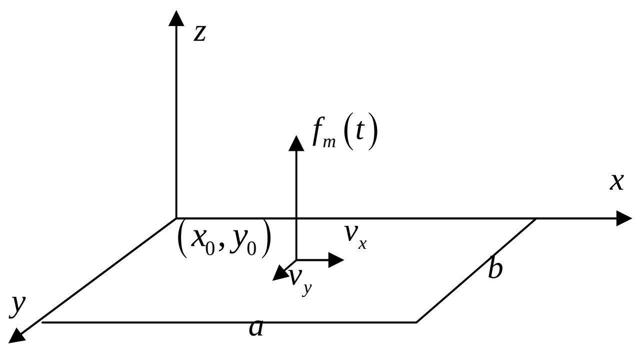

Figure 2. Rectangular plate excited by a harmonic moving force

Using the orthogonal property and assuming proportional damping in the forced vibrating system, substitute Eq. (2-5) into Eq. (1), we obtain the normalized equation of transverse displacement

$$\ddot{W}_{mn} + 2\xi_{mn}\omega_{mn}\dot{W}_{mn} + \omega_{mn}^2 W_{mn} = F_{mn}, \tag{6}$$

where ξ_{mn} is the generalized damping factor defined by

$$\xi_{mn} = c_d / 2\rho h\omega_{mn}. \tag{7}$$

ω_{mn} is the generalized natural frequency defined by

$$\omega_{mn}^2 = \frac{1}{m_{mn}}\int_0^a\int_0^b \nabla^4\Phi_{mn}(x,y)\times\Phi_{mn}(x,y)\,dydx, \tag{8}$$

F_{mn} is the normalized force defined by

$$F_{mn} = \frac{1}{m_{mn}} f_m(t)\Phi_{mn}(x_0 + v_x t, y_0 + v_y t), \tag{9}$$

m_{mn} is the generalized mass of the rectangular plate defined by

$$m_{mn} = \int_0^a\int_0^b \rho h\Phi_{mn}^2(x,y)\,dydx, \tag{10}$$

For a lightly damped system ($\xi_{mn} < 1$), we solve Eq. (4) in time domain by Duhamel integral [10]. Then the displacement coefficient W_{mn} is given by

$$W_{mn} = \exp(-\xi_{mn}\omega_{mn}t)(a_{mn}\sin\varpi_{mn}t + b_{mn}\cos\varpi_{mn}t)$$
$$+\frac{1}{\varpi}\int_0^t F_{mn}\exp\left[-\xi_{mn}\omega_{mn}(t-\tau)\right]\sin\varpi(t-\tau)\,d\tau, \tag{11}$$

where ϖ is the generalized natural frequency of damped free vibration defined by

$$\varpi = \omega_{mn}\sqrt{1-\xi_{mn}^2}\,, \tag{12}$$

the parameters a_{mn} and b_{mn} can be obtained from the initial transverse displacement $w(x,y,0)$ and the initial velocity $\dot{w}(x,y,0)$

$$a_{mn} = \frac{\int_0^a\int_0^b \left[\dot{w}(x,y,0)+2\xi_{mn}\omega_{mn}w(x,y,0)\right]\Phi_{mn}(x,y)\,dydx}{\varpi\int_0^a\int_0^b \Phi_{mn}^2(x,y)\,dydx}, \tag{13}$$

$$b_{mn} = \frac{\int_0^a\int_0^b w(x,y,0)\Phi_{mn}(x,y)\,dydx}{\int_0^a\int_0^b \Phi_{mn}^2(x,y)\,dydx}. \tag{14}$$

Consider a case of a harmonic point force moves at speed of v_x along with the x direction from the initial location (x_0, y_0), the moving force $f_m(t)$ can be written, in terms of the mass of the moving force defined by, as

$$f_m(x,y,t) = f_0 - \mu_f\left(\frac{\partial^2 w}{\partial x^2}v_x^2 + 2\frac{\partial^2 w}{\partial x\partial t}v_x + \frac{\partial^2 w}{\partial t^2}\right), \tag{15}$$

where g is the acceleration due to gravity, μ_f is the mass ratio be the ratio of the mass due to the moving force to the rectangular plate defined by $\mu_f = |f_0/g|$. So, the normalized force is expressed as

$$F_{mn}^* = F_{mn} - \frac{\mu_f\Phi_{mn}}{m_{mn}}\sum_{m=1}^{\infty}\sum_{n=1}^{\infty}\left[v_x^2\frac{\partial^2\Phi_{mn}}{\partial x^2}W_{mn} + 2v_x\frac{\partial\Phi_{mn}}{\partial x}\dot{W}_{mn} + \Phi_{mn}\ddot{W}_{mn}\right]. \tag{16}$$

Truncate the indices m and n after m_u and n_u terms, respectively, Eq. (6) is expressed in matrix form as

$$\left([I]+[M_m]\right)\{\ddot{Q}\} + \left([C_d+[C_m]]\right)\{\dot{Q}\} + \left([K_d]+[K_m]\right)\{Q\} = \{F\}, \tag{17}$$

where $[I]$ is the identity matrix which results from normalization by the generalized mass m_{mn} of the plate, the vector $\{Q\}$ is composed by the displacement coefficient W_{mn} defined by

$$\{Q\} = \left[W_{11},\cdots,W_{1n_u},\cdots,W_{m_u1},\cdots,W_{m_un_u}\right]^T, \tag{18}$$

$[M_m]$ is the generalized mass matrix defined by

$$[M_m] = \mu_F \begin{bmatrix} \frac{\Phi_{11}^2}{m_{11}} & \cdots & \frac{\Phi_{11}\Phi_{1n_u}}{m_{11}} & \cdots & \frac{\Phi_{11}\Phi_{m_u1}}{m_{11}} & \cdots & \frac{\Phi_{11}\Phi_{m_un_u}}{m_{11}} \\ \cdots & \cdots & \cdots & \cdots & \cdots & \cdots & \cdots \\ \frac{\Phi_{1n_u}\Phi_{11}}{m_{1n_u}} & \cdots & \frac{\Phi_{1n_u}^2}{m_{1n_u}} & \cdots & \frac{\Phi_{1n_u}\Phi_{m_u1}}{m_{1n_u}} & \cdots & \frac{\Phi_{1n_u}\Phi_{m_un_u}}{m_{1n_u}} \\ \cdots & \cdots & \cdots & \cdots & \cdots & \cdots & \cdots \\ \frac{\Phi_{m_u1}\Phi_{11}}{m_{m_u1}} & \cdots & \frac{\Phi_{m_u1}\Phi_{1n_u}}{m_{m_u1}} & \cdots & \frac{\Phi_{m_u1}^2}{m_{m_u1}} & \cdots & \frac{\Phi_{m_u1}\Phi_{m_un_u}}{m_{m_u1}} \\ \cdots & \cdots & \cdots & \cdots & \cdots & \cdots & \cdots \\ \frac{\Phi_{m_un_u}\Phi_{11}}{m_{m_un_u}} & \cdots & \frac{\Phi_{m_un_u}\Phi_{1n_u}}{m_{m_un_u}} & \cdots & \frac{\Phi_{m_un_u}\Phi_{m_u1}}{m_{m_un_u}} & \cdots & \frac{\Phi_{m_un_u}^2}{m_{m_un_u}} \end{bmatrix}, \tag{19}$$

$[C_d]$ and $[C_m]$ are the generalized damping matrices defined by

$$[C_d] = 2 \begin{bmatrix} \xi_{11}\omega_{11} & & & & & & \\ & \cdots & & & & & \\ & & \xi_{1n_u}\omega_{1n_u} & & & & \\ & & & \cdots & & & \\ & & & & \xi_{m_u1}\omega_{m_u1} & & \\ & & & & & \cdots & \\ & & & & & & \xi_{m_un_u}\omega_{m_un_u} \end{bmatrix}, \tag{20}$$

$$[C_m] = 2v_x\mu_F \begin{bmatrix} \frac{\Phi_{11}\Phi'_{11}}{m_{11}} & \cdots & \frac{\Phi_{11}\Phi'_{1n_u}}{m_{11}} & \cdots & \frac{\Phi_{11}\Phi'_{m_u1}}{m_{11}} & \cdots & \frac{\Phi_{11}\Phi'_{m_un_u}}{m_{11}} \\ \cdots & \cdots & \cdots & \cdots & \cdots & \cdots & \cdots \\ \frac{\Phi_{1n_u}\Phi'_{11}}{m_{1n_u}} & \cdots & \frac{\Phi_{1n_u}\Phi'_{1n_u}}{m_{1n_u}} & \cdots & \frac{\Phi_{1n_u}\Phi'_{m_u1}}{m_{1n_u}} & \cdots & \frac{\Phi_{1n_u}\Phi'_{m_un_u}}{m_{1n_u}} \\ \cdots & \cdots & \cdots & \cdots & \cdots & \cdots & \cdots \\ \frac{\Phi_{m_u1}\Phi'_{11}}{m_{m_u1}} & \cdots & \frac{\Phi_{m_u1}\Phi'_{1n_u}}{m_{m_u1}} & \cdots & \frac{\Phi_{m_u1}\Phi'_{m_u1}}{m_{m_u1}} & \cdots & \frac{\Phi_{m_u1}\Phi'_{m_un_u}}{m_{m_u1}} \\ \cdots & \cdots & \cdots & \cdots & \cdots & \cdots & \cdots \\ \frac{\Phi_{m_un_u}\Phi'_{11}}{m_{m_un_u}} & \cdots & \frac{\Phi_{m_un_u}\Phi'_{1n_u}}{m_{m_un_u}} & \cdots & \frac{\Phi_{m_un_u}\Phi'_{m_u1}}{m_{m_un_u}} & \cdots & \frac{\Phi_{m_un_u}\Phi'_{m_un_u}}{m_{m_un_u}} \end{bmatrix}, \tag{21}$$

$[K_d]$ and $[K_m]$ are the generalized stiffness matrices defined by

$$[K_d] = \begin{bmatrix} \omega_{11}^2 & & & & & & \\ & \cdots & & & & & \\ & & \omega_{1n_u}^2 & & & & \\ & & & \cdots & & & \\ & & & & \omega_{m_u 1}^2 & & \\ & & & & & \cdots & \\ & & & & & & \omega_{m_u n_u}^2 \end{bmatrix}, \tag{22}$$

$$[K_m] = \mu_F v_x^2 \begin{bmatrix} \frac{\Phi_{11}\Phi''_{11}}{m_{11}} & \cdots & \frac{\Phi_{11}\Phi''_{1n_u}}{m_{11}} & \cdots & \frac{\Phi_{11}\Phi''_{m_u 1}}{m_{11}} & \cdots & \frac{\Phi_{11}\Phi''_{m_u n_u}}{m_{11}} \\ \cdots & \cdots & \cdots & \cdots & \cdots & \cdots & \cdots \\ \frac{\Phi_{1n_u}\Phi''_{11}}{m_{1n_u}} & \cdots & \frac{\Phi_{1n_u}\Phi''_{1n_u}}{m_{1n_u}} & \cdots & \frac{\Phi_{1n_u}\Phi''_{m_u 1}}{m_{1n_u}} & \cdots & \frac{\Phi_{1n_u}\Phi''_{m_u n_u}}{m_{1n_u}} \\ \cdots & \cdots & \cdots & \cdots & \cdots & \cdots & \cdots \\ \frac{\Phi_{m_u 1}\Phi''_{11}}{m_{m_u 1}} & \cdots & \frac{\Phi_{m_u 1}\Phi''_{1n_u}}{m_{m_u 1}} & \cdots & \frac{\Phi_{m_u 1}\Phi''_{m_u 1}}{m_{m_u 1}} & \cdots & \frac{\Phi_{m_u 1}\Phi''_{m_u n_u}}{m_{m_u 1}} \\ \cdots & \cdots & \cdots & \cdots & \cdots & \cdots & \cdots \\ \frac{\Phi_{m_u n_u}\Phi''_{11}}{m_{m_u n_u}} & \cdots & \frac{\Phi_{m_u n_u}\Phi''_{1n_u}}{m_{m_u n_u}} & \cdots & \frac{\Phi_{m_u n_u}\Phi''_{m_u 1}}{m_{m_u n_u}} & \cdots & \frac{\Phi_{m_u n_u}\Phi''_{m_u n_u}}{m_{m_u n_u}} \end{bmatrix}, \tag{23}$$

$\{F\}$ is the generalized force vector defined by

$$\{F\} = \left[F_{11}, \cdots, F_{1n_u}, \cdots, F_{m_u 1}, \cdots, F_{m_u n_u}\right]^T, \tag{24}$$

where $\Phi_{ij} = \Phi_{ij}\left(v_x t, y_0\right)$, $\Phi'_{ij} = \dfrac{\partial \Phi_{ij}}{\partial x}$, $\Phi''_{ij} = \dfrac{\partial^2 \Phi_{ij}}{\partial x^2}$.

The mode shape function $\Phi_{mn}(x, y)$ of the rectangular plate is given by [9]

$$\Phi_{mn}(x, y) = X_m(x) Y_n(y), \tag{25}$$

where $X_m(x)$ and $Y_n(y)$ are taken to be the mode shapes of the associated un-damped beams, having the same boundary conditions as the plate in x and y directions, respectively. Consider a un-damped beam of length l, the governing equation is given by [9]

$$EI \frac{\partial^4 w(x, y)}{\partial x^4} + \rho_b \frac{\partial^2 w(x, t)}{\partial t^2} = 0 \tag{26}$$

where EI is the flexural rigidity defined by $EI = \left(1 - \mu^2\right) D$, ρ_b is the mass per unit length. Suppose $w(x,t) = X(x)\sin(\omega t)$, we obtain

$$X_m(x) = A_{1m} \sin \alpha_m x + A_{2m} \cos \alpha_m x + A_{3m} \sinh \alpha_m x + A_{4m} \cosh \alpha_m x, \tag{27}$$

where the parameters A_{1m}, A_{2m}, A_{3m} and A_{4m} are determined by boundary conditions respectively, α_m is the eigenvalue of the m^{th} mode defined by

$$\alpha_m = \rho_b S_b \omega_m^2 / EI \,, \tag{28}$$

m is positive integer, S_b is the beam section area, ω_m is the m^{th} mode eigenfrequency.

For a rectangular plate with elastic support as shown in Fig.1, the boundary conditions is given by

(1) at edge $y = 0$

$$\begin{cases} R_0 \dfrac{\partial w}{\partial y} - D\left(\dfrac{\partial^2 w}{\partial y^2} + \mu \dfrac{\partial^2 w}{\partial x^2}\right) = 0, \\ T_0 w + D\dfrac{\partial^3 w}{\partial y^3} + D(2-\mu)\dfrac{\partial^3 w}{\partial x^2 \partial y} = 0, \end{cases} \tag{29}$$

(2) at edge $y = b$

$$\begin{cases} R_b \dfrac{\partial w}{\partial y} + D\left(\dfrac{\partial^2 w}{\partial y^2} + \mu \dfrac{\partial^2 w}{\partial x^2}\right) = 0, \\ T_b w - D\dfrac{\partial^3 w}{\partial y^3} + D(2-\mu)\dfrac{\partial^3 w}{\partial x^2 \partial y} = 0, \end{cases} \tag{30}$$

(3) at edge $x = 0$

$$\begin{cases} R_1 \dfrac{\partial w}{\partial x} - D\left(\dfrac{\partial^2 w}{\partial x^2} + \mu \dfrac{\partial^2 w}{\partial y^2}\right) = 0, \\ T_1 w + D\dfrac{\partial^3 w}{\partial x^3} + D(2-\mu)\dfrac{\partial^3 w}{\partial x \partial y^2} = 0, \end{cases} \tag{31}$$

(4) at edge $x = a$

$$\begin{cases} R_a \dfrac{\partial w}{\partial x} + D\left(\dfrac{\partial^2 w}{\partial x^2} + \mu \dfrac{\partial^2 w}{\partial y^2}\right) = 0, \\ T_a w - D\dfrac{\partial^3 w}{\partial x^3} + D(2-\mu)\dfrac{\partial^3 w}{\partial x \partial y^2} = 0, \end{cases} \tag{32}$$

where the parameters R_0, T_0, R_b, T_b, R_1, T_1, R_a and T_a are stiffness of the rotational springs and the translational springs at every side, respectively.

For the beam modal shape function in Eq. (25), we treat $X_m(x)$ as a strip element of the plate. So, the flexural rigidity EI of the beam can be replaced by $D(1-\mu^2)$. According to Eq. (29) and (30), we obtain the following homogenous linear equation [11]

$$\begin{bmatrix} -u^3 & R_{T0} & u^3 & R_{T0} \\ R_{R0} & u & R_{R0} & -u \\ u^3 \cos u + R_{Tb} \sin u & -u^3 \sin u + R_{Tb} \cos u & -u^3 \cosh u + R_{Tb} \sinh u & -u^3 \sinh u + R_{Tb} \cosh u \\ -u \sin u + R_{Rb} \cos u & -u \cos u - R_{Rb} \sin u & u \sinh u + R_{Rb} \cosh u & u \cosh u - R_{Rb} \sinh u \end{bmatrix} \times \begin{bmatrix} A_{1m} \\ A_{2m} \\ A_{3m} \\ A_{4m} \end{bmatrix} = \begin{bmatrix} 0 \\ 0 \\ 0 \\ 0 \end{bmatrix}, \tag{33}$$

where $R_{T0} = T_0 a^3 / EI$, $R_{Tb} = T_b a^3 / EI$, $R_{R0} = R_0 a / EI$, $R_{Rb} = R_b a / EI$, $u = \sqrt[4]{\rho S \omega_m^2 a^4 / EI}$.
According to Eq. (33), the eigenfunction is given by

$$u^8(1-\cos u \cosh u) + u^7\left[-(R_{R0}+R_{Rb})(\sin u \cosh u + \cos u \sinh u)\right] +$$
$$u^6(-2R_{R0}R_{Rb} \sin u \sinh u) + u^5\left[(R_{T0}+R_{Tb})(\cos u \sinh u - \sin u \cosh u)\right] +$$

$$u^4\left[\left(R_{T0}R_{R0}+R_{Tb}R_{Rb}\right)\left(1+\cos u\cosh u+2\left(R_{T0}R_{Rb}+R_{Tb}R_{Rb}\right)\cos u\cosh u\right)\right]+$$
$$u^3\left[R_{R0}R_{Rb}\left(R_{T0}+R_{Tb}\right)\left(\cos u\sinh u+\sin u\cosh u\right)\right]+u^2\left(2R_{T0}R_{Tb}\sin u\sinh u\right)+$$
$$u\left[R_{T0}R_{Tb}\left(R_{R0}+R_{Rb}\right)\left(\sin u\cosh u-\cos u\sinh u\right)\right]+R_{T0}R_{Tb}R_{R0}R_{Rb}\left(1-\cos u\cosh u\right)=0\,. \quad (34)$$

Solving Eq. (34), we obtain the positive eigenvalues $u_1,u_2,\cdots u_m$. Since the natural frequency of beam can be expressed as

$$\omega_m=u_m^2\sqrt{EI/\rho_b Sa^4}\ , \quad (35)$$

the modal shape function in x direction $X_m\left(x\right)$ can be obtained according to Eq. (27).

Similarly, we can suppose

$$Y_n\left(y\right)=B_{1n}\sin\beta_n y+B_{2n}\cos\beta_n y+B_{3n}\sinh\beta_n y+B_{4n}\cosh\beta_n y\,, \quad (36)$$

where the parameters B_{1n}, B_{2n}, B_{3n} and B_{4n} are determined by boundary conditions, respectively, β_n is the eigenvalue of the n^{th} mode, n is positive integer. Using the method mentioned above, we obtain the modal shape function $Y_n\left(y\right)$ in y direction.

Once we obtain the mode shape function, the transverse displacement $w\left(x,y,t\right)$ of the rectangular plate can be obtain by solving Eq. (17). Especially, for the case of low mass ratio, μ_F can be ignored. Thus, the transverse displacement of the rectangular plate is further simplified to

$$w\left(x,y,t\right)=\sum_{m=1}^{\infty}\sum_{n=1}^{\infty}\frac{f_0\Phi_{mn}\left(x,y\right)}{\varpi m_{mn}}\int_o^t\exp\left[-\xi_{mn}\omega_{mn}\left(t-\tau\right)\right]\Phi_{mn}\left(v_x\tau,y_0\right)\sin\left[\varpi\left(t-\tau\right)\right]d\tau\,. \quad (37)$$

For a rectangular plate in an infinite baffle as shown in Fig.3, the radiated sound pressure from the plate can be obtained by evaluating the Rayleigh surface integral where each element area on the plate is treated as a simple point sound source and its contribution is added with an appreciate time delay. The sound pressure at observation location $P\left(x_P,y_P,z_P\right)$ is given by [12]

$$p\left(Q\right)=\frac{j\omega\rho_0}{2\pi}\int_S\frac{e^{-jkr}}{r}\dot{w}\left(P\right)dS\ , \quad (38)$$

where ρ_0 is the air density, S is the surface area of the plate, r is the distance between the observation location and the infinitesimal element on the plate.

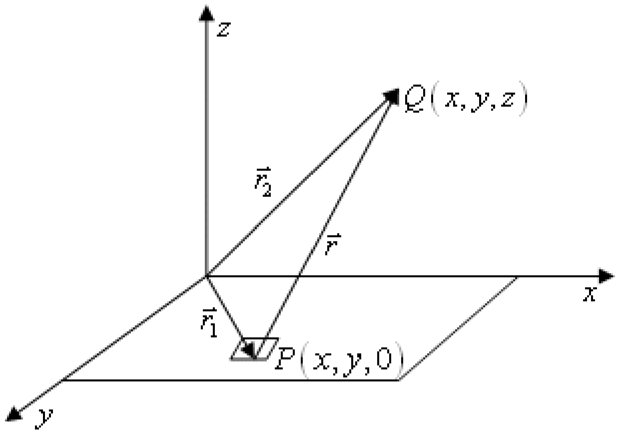

Figure.3 Coordinate system for evaluation of structural sound pressure

The structural sound intensity at the observation location Q is [12]

$$I(Q)=\frac{1}{2}\mathrm{Re}\left[p(Q)v^*(Q)\right], \tag{39}$$

where $v(Q)$ is the velocity of acoustic medium at the location Q, * denotes complex conjugate. The sound power radiated into the semi-infinite space above the plate is given by

$$W=\int_{S'} I(Q)dS', \tag{40}$$

where S' is an arbitrary surface which covers area S.

According to Eq. (38) and (39), Eq. (40) takes the form

$$W=\frac{\omega\rho_0}{4\pi}\int_{S'}\int_S \mathrm{Re}\left[\dot{w}(P)\frac{je^{-jkr}}{r}v^*(Q)\right]dSdS'. \tag{41}$$

Since $\mathrm{Re}\{J\}=(J+J^*)/2$, where J is a complex function, we note that

$$\mathrm{Re}\left[\dot{w}(P)\frac{je^{-jkr}}{r}v^*(Q)\right]=\frac{1}{2}\left[\dot{w}(P)\left(\frac{je^{-kr}}{r}\right)v^*(Q)+\dot{w}^*(P)\left(\frac{-je^{-kr}}{r}\right)v(Q)\right]$$

$$=\frac{1}{2}\left[\dot{w}(P)\left(\frac{\sin\theta+i\cos\theta}{r}\right)v^*(Q)+\dot{w}^*(P)\left(\frac{\sin\theta-i\cos\theta}{r}\right)v(Q)\right]. \tag{42}$$

When we suppose S' to S, due to the reciprocity relationship between $\vec{r}_1$ and $\vec{r}_2$ (Fig.3), $v(Q)=\dot{w}(Q)$. Eq. (42) is simplified as

$$\mathrm{Re}\left[\dot{w}(P)\frac{je^{-jkr}}{r}\dot{w}^*(Q)\right]=\dot{w}(P)\frac{\sin(kr)}{r}\dot{w}^*(Q). \tag{43}$$

Then Eq. (41) is given by

$$W=\frac{\omega\rho_0}{4\pi}\int_0^b\int_0^a\left[\int_0^b\int_0^a \dot{w}(P)\frac{\sin(kr)}{r}\dot{w}^*(Q)dxdy\right]dx'dy'. \tag{44}$$

When the plate is divided into N elements, Eq. (44) is approximated by a finite series

$$W \approx \frac{\omega\rho_0}{4\pi}\sum_{i=1}^{N}\sum_{j=1}^{N}\dot{w}(\vec{r}_i)\,\dot{w}^*(\vec{r}_j)\frac{\sin kr}{r}(\Delta S)^2, \tag{45}$$

where $\vec{r}_i$ and $\vec{r}_j$ are the position vectors of the center point of two elements.

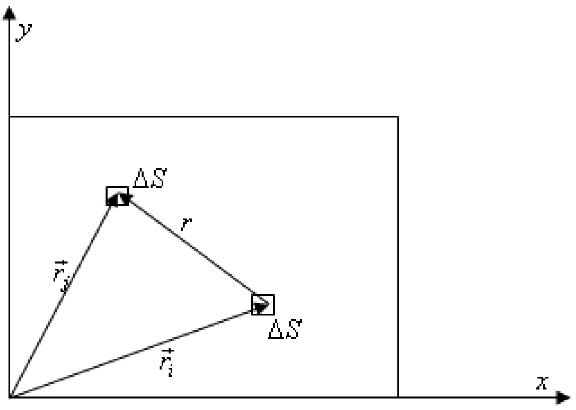

Figure.4 Discretization of the Rectangular Plate Surface

When we define the velocity matrix as $\dot{w} = (\dot{w}_1, \cdots, \dot{w}_i, \cdots, \dot{w}_N)^T$, where T denotes transposition, W is expressed as

$$W = \dot{w}^H Z \dot{w}, \tag{46}$$

where H denotes complex conjugate and transposition, Z is the resistance matrix defined by

$$Z = \frac{\omega^2\rho_0 S^2}{4\pi N^2 c_0}\begin{bmatrix} 1 & \frac{\sin kr_{1,2}}{kr_{1,2}} & \cdots & \frac{\sin kr_{1,N}}{kr_{1,N}} \\ \frac{\sin kr_{2,1}}{kr_{2,1}} & 1 & \cdots & \frac{\sin kr_{2,N}}{kr_{2,N}} \\ \vdots & \vdots & \ddots & \vdots \\ \frac{\sin kr_{N,1}}{kr_{N,1}} & \frac{\sin kr_{N,2}}{kr_{N,2}} & \cdots & 1 \end{bmatrix}. \tag{47}$$

where c_0 is the sound velocity in air.

In free sound field, according to [12], the radiated sound pressure level L_p is given by

$$L_p = 10\lg\frac{W}{W_0} - 10\lg S - 10\lg\frac{400}{\rho_0 c_0}, \tag{48}$$

where W_0 is reference sound power and defined by 10^{-12} Watt.

3. Numerical Results and Discussions

Consider a flat rectangular steel plate ($E = 2.1\times10^{11}Pa$, $\rho = 7800kg/m^3$, $\mu = 0.28$) of size $0.5\times0.3m$. When the temperature is $20^\circ C$, the properties of air are $\rho_0 = 1.21kg/m^3$ and $c = 343m/s$. The damping coefficients obtained from experiments [15, 16] adopted for the numerical computations are $c_d = \rho h\omega/100\pi$, where h is the plate thickness. Choose the location (0.25, 0.15, 0.005) as the observation location and 50-1000Hz as the frequency range adopted in this numerical calcualtion. The stiffness of all the springs is $50 Newton/m$.

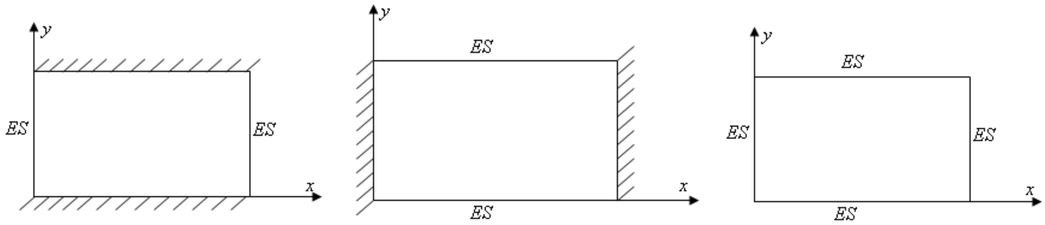

(a) C-ES-C-ES (b) ES-C-ES-C (c) ES-ES-ES-ES

Figure.5 Rectangular plates with elastic support boundary conditions, where C denotes the clamped support, ES denotes the elastic support

Consider a case of low mass ratio, then the mass ratio μ_f can be ignored. We set the magnitude of the harmonic moving force is $F(t) = e^{j\omega t} Newton$. When the force moves at a speed of $v_x = 0.5 m/s$ from the initial location (0, 0.1) along with the line $y = 0.1$, the radiated sound pressure level from the plates at the observation point is shown in Fig.6.

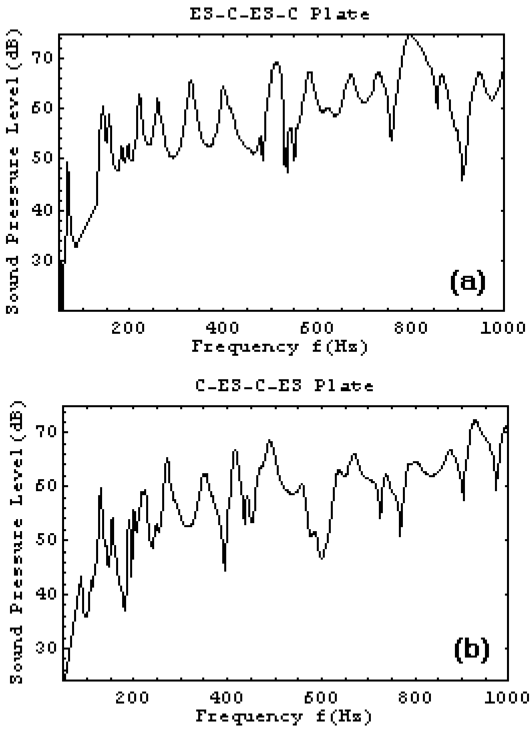

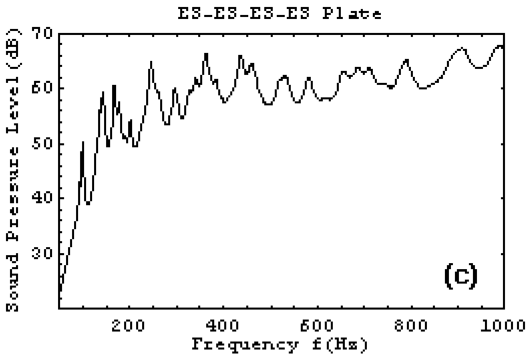

Figure.6 Radiated sound pressure level from the rectangular plates in a case of low mass ratio: (a) the sound pressure level radiated from the ES-C-ES-C plate, (b) the sound pressure level radiated from the C-ES-C-ES plate, (c) the sound pressure level radiated from the ES-ES-ES-ES plate.

Comparing the curve of the sound-pressure-level versus frequency, the radiated sound pressure level from the ES-ES-ES-ES plate (Fig.6 c) is flatter than from the ES-C-ES-C plate (Fig.6 a) and the C-ES-C-ES plate (Fig.6 b). Especially, when the frequency is higher than 400Hz, the fluctuation of the radiated sound pressure level from the ES-ES-ES-ES plate (Fig.6 c) is quite small. Notice that, the value of the radiated sound pressure level from the ES-ES-ES-ES plate (Fig.6 c) is higher in the frequency range of 400-1000Hz. When the boundary condition at the end of the plate is changed from clamped-support to elastic-support (Fig.6 a, c), the frequencies, which make the radiated sound pressure level from the ES-C-ES-C plate to maximum or minimum value, does not appear. Moreover, when the frequency is lower than 200Hz, the radiated sound pressure level from the ES-ES-ES-ES plate is higher than from the ES-C-ES-C plate. Changing the boundary condition at the side of the plate from clamped-support to elastic-support (Fig.6 b, c), when the frequency is in the range of 200-400Hz, the radiated sound pressure level from the C-ES-C-ES plate is quite lower than from the ES-ES-ES-ES plate. Notice that, comparing the radiated sound pressure level from the ES-C-ES-C plate and the C-ES-C-ES plate (Fig.6 a, b), the curve of the former is also flatter than the later. We find that the elastic support has great effect on the radiation sound. More elastic-support in the boundary condition of the plate edge make the curve of the sound-pressure-level versus frequency flatter.

Because the plate thickness variation will cause the mode density variation, for investigating the effect of the mode density on the modulated radiated sound roughness from the plate, for further investigating the effect of the elastic support on the radiation sound, we consider the plate thickness is variable in the range of 0.3-1.5mm. The radiated sound pressure level from the rectangular plates is shown in Fig.7.

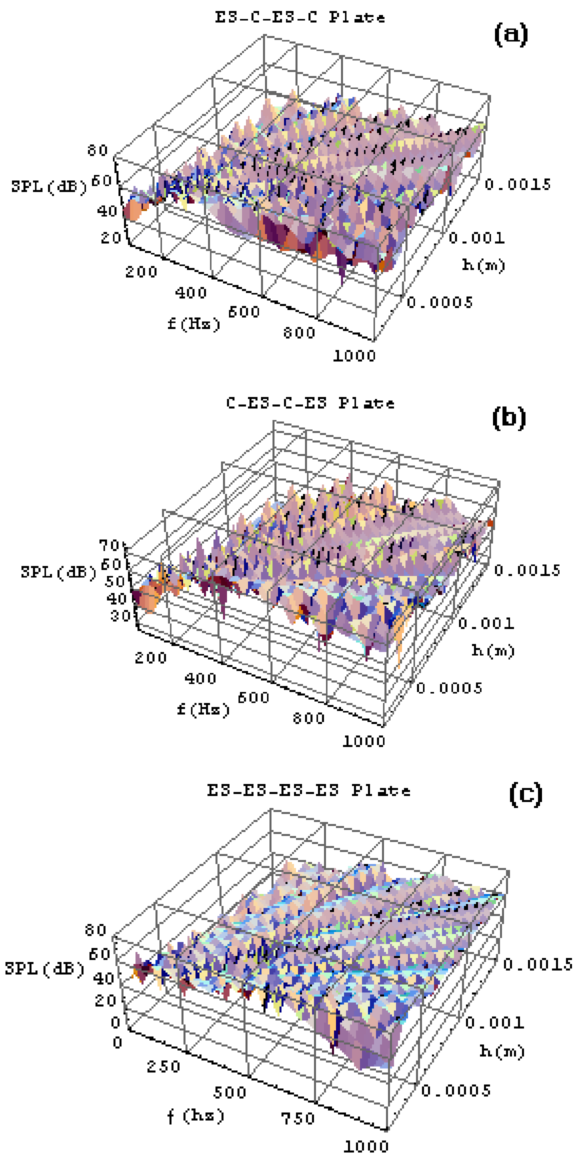

Figure.7 Sound pressure level radiated from the rectangular plates when the plate thickness is variable in the case of low mass ratio: (a) the sound pressure level radiated from the ES-C-ES-C plate (b) the sound pressure level radiated from the C-ES-C-ES plate, (c) the sound pressure level radiated from the ES-ES-ES-ES plates

When the plate thickness increases, the structural mode density becomes sparse [17]. With the plate thickness increasing, although the elastic support has less effect on the radiated sound pressure level from the plate, there are still some differences. When changing the boundary condition at the end of the plate from clamped-support to elastic-support, the frequency range, which make the radiated sound pressure level from the ES-ES-ES-ES plate higher than from the ES-C-ES-C plate (Fig.7 a, c) in low frequency range, becomes wider with the plate thickness increasing. Similarly, when change the boundary condition at the side of the plate from clamped-support to elastic-support, the frequency range, which make the radiated sound pressure level from the ES-ES-ES-ES plate higher than from the C-ES-C-ES plate (Fig.7b, c) in middle frequency range, also becomes wider with the plate thickness increasing.

Comparing Fig.6 and Fig.7, we find the same conclusion with the frequency increasing. Whatever the plate mode density is, more elastic-support boundary condition makes the fluctuation of the radiated sound pressure level from the plate less. However, there are less frequencies, which make the radiated sound pressure level from the plate to maximum value, appears with the plate thickness increasing.

When in a case of high mass ratio, the effect of the moving force speed should be taken into account. For investigating the effect of the moving force on the radiated sound in the case of high mass ratio, we choose two different moving force speeds.

Suppose the magnitude of the moving force is $f_0 = 10e^{j\omega t} newton$, when the force moves at low speed of $v_x = 0.5m/s$ from the initial location (0, 0.1) along with the line $y = 0.1$, the radiated sound pressure level from the rectangular plates is shown in Fig.8.

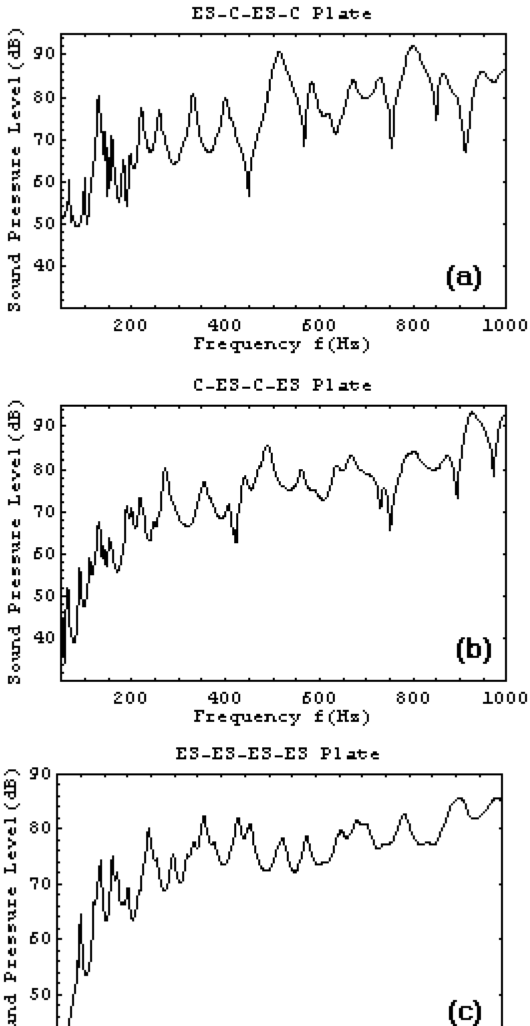

Figure.8 Sound pressure level radiated from the rectangular plates in the case of high mass

ratio case when the force moves at a low speed: (a) the sound pressure level radiated from the ES-C-ES-C plate, (b) the sound pressure level radiated from the C-ES-C-ES plate, (c) the sound pressure level radiated from the ES-ES-ES-ES plate

In the case of high mass ratio, comparing Fig.6 and Fig.8, the curve of the sound-pressure-level versus frequency is quite different from the one in the case of low mass ratio. Fewer frequencies make the sound pressure level to maximum value in the case of high mass ratio whatever the boundary condition is. However, the fluctuation of the radiated sound pressure level form the plate is larger than in the case of low mass ratio. Notice that, more the edge of the plate is elastically supported, the mass ratio has fewer effect on the sound radiated from the plate. The effect of the elastic support on the radiated sound from the plate is also different from in the case of low mass ratio. There is no difference for the effect of elastic support on the sound radiated from the ES-ES-ES-ES plate (Fig.8 c). However, when the boundary condition at the end of the plate is changed from elastic-support to clamped-support (Fig.8 a), the curve of the sound-pressure-level versus frequency is quite flatter in low frequency range than the one in the case of low mass ratio. Similarly, when changing the boundary condition at the side of the plate from elastic-support to clamped-support, similar phenomenon is observed.

In order to investigate the effect of the speed of the moving force, we use the same moving force chose in the case of high mass ratio. When the force moves at high speed of $v_x = 5m/s$ from the initial location (0, 0.1) along with the line $y = 0.1$, the radiated sound pressure level from the rectangular plates is shown in Fig.9.

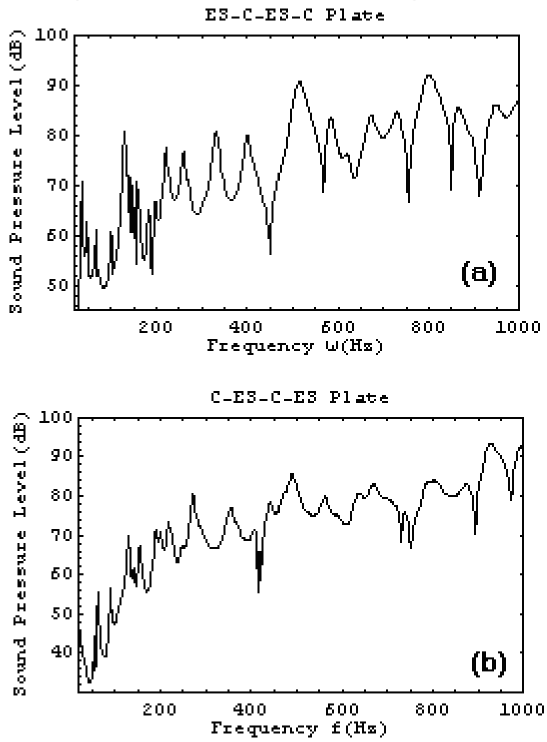

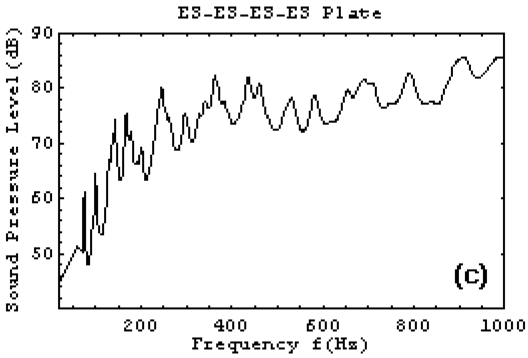

Figure.9 Sound pressure level radiated from the rectangular plates in the case of high mass ratio when the force moves at high speed: (a) the sound pressure level radiated from the ES-C-ES-C plate, (b) the sound pressure level radiated from the C-ES-C-ES plate, (c) the sound pressure level radiated from the ES-ES-ES-ES plate.

Comparing Fig.8 and Fig.9, we find the effect of the high speed of the moving force on the radiated sound from the plates. In the low frequency range of 20-100Hz, the sound pressure level radiated from the ES-C-ES-C plate and the ES-ES-ES-ES plate (Fig.9 a, c) is higher than in the case of low speed of the moving force. However, the sound pressure level radiated from the C-ES-C-ES plate (Fig.9 b) is lower than in the case of low speed in the same frequency range. Notice that, although the curve of the sound-pressure-level versus frequency is quite similar with the one in the case of low speed when the frequency is higher than 100Hz, the radiated sound pressure level from the plate is always higher than the one on the case of low speed of the moving force. There is also some difference of the effect of the elastic-support on the sound radiated from the plate. When boundary condition at the side of the plate is elastic-support (Fig.9 a, c), the sound pressure level has less fluctuation in the low frequency range. On the other hand, when the boundary condition at the end of the plate is elastic-support (Fig.9 b, c), the sound pressure level has less fluctuation in the high frequency range. Notice that, in the low frequency range, more frequencies make the radiated sound pressure level from the plates to maximum value whatever the boundary condition is.

For further investigating the effect of the speed of the moving force on the sound radiated from the plate, we suppose the plate thickness is variable in the range of 0.3-1.5mm. The radiated sound pressure level from the rectangular plates at low speed and high speed, respectively, is shown in Fig.10.

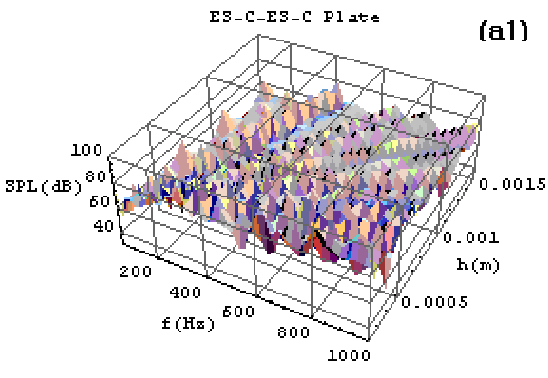

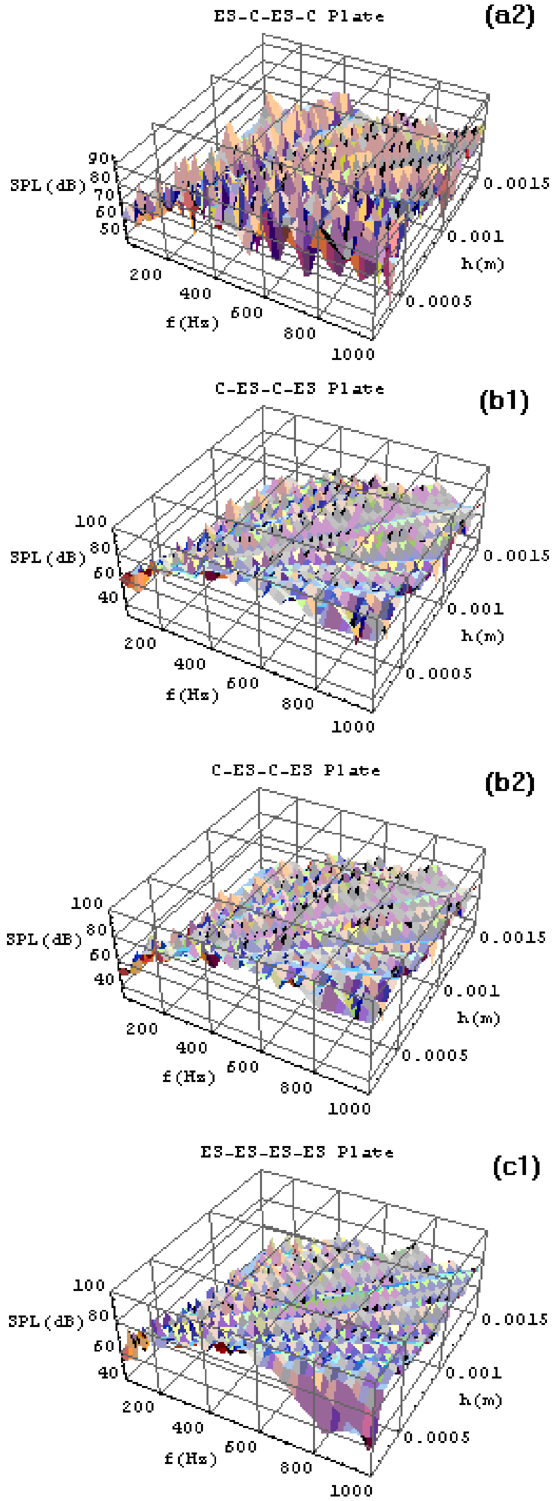
ES-C-ES-C Plate
(a2)
SPL (dB)
90
80
70
60
50
200
400
600
800
1000
f (Hz)
0.0015
0.001
h (m)
0.0005
C-ES-C-ES Plate
(b1)
SPL (dB)
100
80
60
40
200
400
600
800
1000
f (Hz)
0.0015
0.001
h (m)
0.0005
C-ES-C-ES Plate
(b2)
SPL (dB)
100
80
60
40
200
400
600
800
1000
f (Hz)
0.0015
0.001
h (m)
0.0005
ES-ES-ES-ES Plate
(c1)
SPL (dB)
100
80
60
40
200
400
600
800
1000
f (Hz)
0.0015
0.001
h (m)
0.0005

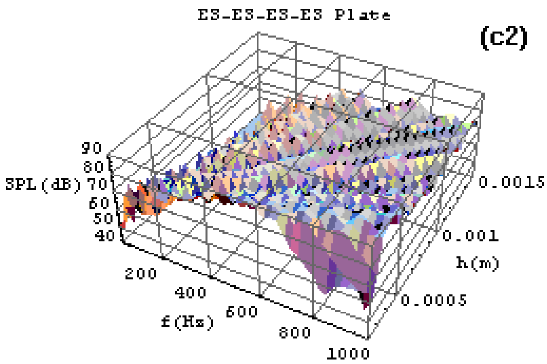

Figure.10 Radiated sound pressure level from the rectangular plates in the case of high mass ratio when the plate thickness is variable: (a1) the radiated sound pressure level from the ES-C-ES-C plate when the force moves at low speed of $v_x = 0.5m/s$, (a2) the radiated sound pressure level from the ES-C-ES-C plate when the force moves at high speed of $v_x = 5m/s$, (b1) the radiated sound pressure level from the C-ES-C-ES plate when the force moves at low speed of $v_x = 0.5m/s$, (b2) the radiated sound pressure level from the C-ES-C-ES plate when the force moves at high speed of $v_x = 5m/s$, (c1) the radiated sound pressure level from the ES-ES-ES-ES plate when the force moves at low speed of $v_x = 0.5m/s$, (c2) the radiated sound pressure level from the ES-ES-ES-ES plate when the force moves at high speed of $v_x = 5m/s$.

With the plate thickness increasing, although the speed of the moving force has less effect on the radiated sound from the plates, there are still some differences. In the low frequency range, the value difference between the radiated sound pressure level from the ES-C-ES-C plate and the ES-ES-ES-ES plate (Fig.10 a2, c2) in the case of high speed and in the low speed (Fig.10 a1, c1) becomes fewer with the plate thickness increasing. Similarly, the value difference between the radiated sound pressure level from the C-ES-C-ES plate in the high-speed case (Fig.10 b2) and in the low-speed case (Fig.10 b1) has same trend with the plate thickness increasing.

Comparing Fig.8, Fig.9 and Fig.10, we find that, with the plate thickness increasing, the elastic-support always has great effect on the radiated sound from the plate whatever the speed of the moving force is. When the boundary condition at the side of the plate is the elastic-support, the curve of the sound-pressure-level versus frequency is flatter in low frequency range, which becomes wider with the plate thickness increasing. Similar phenomenon is also observed in the middle frequency range when the boundary condition at the end of the plate is elastic-support with the plate thickness increasing.

4. Conclusions

Using developed analytical method in conjunction with numerical method, the effect of the moving force and the elastic-support on the radiated sound from the rectangular plate is studied in this paper by comparing the different magnitude and moving speed of the force applied on the plate. Based on the Rayleigh integral, the radiated sound pressure level from the ES-C-ES-C plate, the C-ES-C-ES plate and the ES-ES-ES-ES plate are calculated when different forces apply on the plates, respectively. According to the calculation results, the effects of the elastic-support and the moving force on sound radiated from the rectangular plate are revealed, respectively.

In the case of low mass ratio, through calculation results of the radiated sound pressure level from the rectangular plates with elastic support, we get a conclusion that the curve of the sound-pressure-level versus frequency becomes flat when more edge of the plate is elastically supported. The sound pressure level in the case of high mass ratio is also verified this conclusion. In order to investigate the effect of the moving force, we choose two cases of low moving speed and high moving speed, respectively. The calculation results show that the speed of the moving force can change the sound radiated from the plate with elastic support to become flat in special frequency range. The results also show that the plate mode density on the radiated sound from the plates.

References

[1] S.R. Soni, R.K. Sankara. Vibration of non-uniform rectangular plates: a spline technique method of solution. Journal of Sound and Vibration 1974, 35(1): 35-45

[2] C. Filipich, P.A.A. Laura, R.D. Santos. A note on vibration of rectangular plates. Journal of Sound and Vibration 1977, 50(3): 445-454

[3] Mukherjee, M. Mukhopadhyay. Finite element for flexural vibration analysis of plates having various shapes and varying rigidities. Computational Structure 1986, 23(6): 807-812

[4] R.H. Gutierrez, P.A.A. Laura, R.O. Grossi. Vibration of rectangular plates of bi-linearly varying thickness and with boundary conditions. Journal of Sound and Vibration 1981, 75:323-328

[5] Y.K. Cheung, D. Zhou. The free vibration of rectangular plates using a new set of beam function with the Rayleigh-Ritz method. Journal of Sound and Vibration 1999, 223(5): 703-722

[6] J.A. Gabadeyan, S.T. Oni. Dynamic behavior of beams and rectangular plates under moving loads. Journal of Sound and Vibration 1995, 182(5): 677-695

[7] H. Takabatake. Dynamic analysis of rectangular plates with stepped thickness subjected to moving loads additional mass. Journal of Sound and Vibration 1998, 213(5): 829-842

[8] T. Takahagi, M. Nakai, Y. Tamai. Near Field Sound Radiation From Simply Supported Rectangular Plate. Journal of Sound and Vibration, 1995, 185(3):455-471

[9] A.W. Leissa. Vibration of Plates. Washington DC: NASA SP-160. 1969

[10] T.P. Chang, H.C. Chang. Vibration and buckling analysis of rectangular plates with nonlinear elastic end restraints against rotation. International Journal of Solids Structure 1997, 34(18): 2291-2301

[11] W.T. Thomson. Theory of vibration with applications. New Jersey: Prentice Hall. 1972

[12] L. Rayleigh. Theory of Sound (2nd Edition). New York: Dover Publications. 1987

[13] S. Schedin, C. Lambourge, A. Chaigne. Transient sound fields from impacted plates: comparison between numerical simulations and experiments. Journal of Sound and Vibration, 1999, 221(3): 471-490

[14] C.C. Sung, J.T. Jan. The response of and sound power radiated by a clamped rectangular plate. Journal of Sound and Vibration 1997, 207(3): 301-317
[15] T. Takahagi, M. Nakai, Y. Tamai. Near Field Sound Radiation From Simply Supported Rectangular Plate. Journal of Sound and Vibration, 1995, 185(3):455-471
[16] Yuh-Chun Hu, Shyh-Chin Huang. The frequency response and damping effect of three-layer thin shell. Computers and Structures, 2000, 76(5):577-591
[17] G. Xie, D.J. Thompson, C.J.C. Jones. Mode count and modal density of structural systems: relationships with boundary conditions. Journal of Sound and Vibration, 2004, 27(3-5): 621-651

Received: February, 2007